POLITECNICO DI TORINO
Repository ISTITUZIONALE

Non-Intrusive Underwater Measurement of Local Scour Around a Bridge Pier

Original
Non-Intrusive Underwater Measurement of Local Scour Around a Bridge Pier / Poggi, D., KUDRYAVTSEVA MORSE, N.. - In: WATER. - ISSN 2073-4441. - ELETTRONICO. - 11:10(2019). [10.3390/w11102063]

Availability:
This version is available at: 11583/2823172 since: 2020-05-12T18:16:31Z

Publisher:
MDPI

Published
DOI:10.3390/w11102063

Terms of use:

This article is made available under terms and conditions as specified in the corresponding bibliographic description in the repository

Publisher copyright

(Article begins on next page)

07 November 2026

water

MDPI

Article

Non-Intrusive Underwater Measurement of Local Scour Around a Bridge Pier

Davide Poggi * and Natalia O. Kudryavtseva

Department of Environment, Land and Infrastructure Engineering, Politecnico di Torino, Corso Duca degli Abruzzi 24, 10129 Turin, Italy; designbyaspect@yahoo.co.uk

* Correspondence: davide.poggi@polito.it

Received: 24 August 2019; Accepted: 30 September 2019; Published: 2 October 2019



Abstract: A non-intrusive low-cost technique for monitoring the temporal and spatial evolution of the scour hole around bridge piers is presented. The setup for the application of the technique is simple, low-cost and non-intrusive. It couples a line laser source and commercial camera to get a fast and accurate measurement of the whole scour hole in the front and behind the bridge pier. A short campaign of measurements of the scour hole around a bridge pier in clear-water conditions is presented to provide a control test and to show how to apply the new method. Finally, the results are compared with two of the most used equations, for the time evolution of the maximum scour depth in clear-water conditions, to show the effectiveness of the proposed technique.

Keywords: bridge pier scour; new experimental technique

1. Introduction

Scouring at bridge piers and river abutments is one of the main causes of bridge failures, causing major losses to the road networks and rail infrastructures [1–6]. Local scour, which is the purpose of this work, is due to vortices forming at the base of pier impacted by the water current. This process is time-dependent and, despite the research efforts during the last five decades, the time evolution of scour depth remains a subject of concern for hydraulic engineers and researchers. The main problem from the experimental point of view is that this phenomenon requires thorough spatial investigation and continuous monitoring of the morphological characteristics of the riverbed.

In general, the equilibrium between flow erosion capability and the resistance to motion of the bed is gradually reached through the adjustment of the bottom boundary which imposes the depth of scour hole and its three-dimensional shape around the piers [7–9]. While in live-bed conditions this equilibrium is very rapidly achieved and oscillates due to the passage of bed-forms in clear-water conditions the process is rather slow or never reached [10–13]. According to a large number of experimental studies, the equilibrium is reached in finite time [2,14]. However, few authors argue that equilibrium can be reached only asymptotically [15]. Research on local scouring has been made mostly through laboratory experimentation and, in the last decades, a large number of runs have been carried out for evaluating bridge vulnerability to scour under several experimental conditions (pier diameter, water velocity and depth, grain diameter, etc.) [2,9,13–21].

From an engineering point of view, once the design of the pier is done (shape of the pier and its orientation with respect to the flow), and the extreme flow conditions are chosen, the relevant questions are those connected not only with the maximum depth of the scour but also with the shape and dimension of the whole scour hole. Scour and deposition are both central in bridge design. While, as stated above, local scour mechanism is often responsible for bridge failure, the dunes, that grow in the wake of the bridge piers and fed by scoured bed material, are relevant in river control engineering as they can become significant obstacles for the flow downstream of bridges [22]. Very few systematic

studies on dune morphology have been published. Based on a large data set, Oliveto and Hager [22] were able to characterize the dune formation downstream of a bridge pier as a direct consequence of the local scour process. They found that the parameters imposing the dune morphology are the relative pier diameter, densimetric Froude number, wash-out parameter, and relative time. Chavan and Kumar [23] studied the features of dunes downstream of piers and found that the height of deposition increases with downward seepage. Pagliara and Carnacina [24–27] conducted a temporal analysis of dune morphology in the presence of debris accumulations at bridge pier in clear water condition and showed that the dune could be eroded under a given condition of high occlusion or high flow intensity.

Much more data and laboratory experiments are needed to improve knowledge on dune evolution principles and to assess and validate new theoretical and numerical models. This clashes with the experimental difficulties in measuring, with an appropriate time and spatial resolution, the shape of the scour, and the resulting dune, in bed conditions that can initially vary very quickly and, later on in time, on very large surfaces. Although very advanced and expensive equipment is used in the laboratory to study the flow field above an erodible bed [28–33] the current technology for measuring its space-time evolution is dramatically lacking. In fact, in the case of the scour hole, the depth is often measured, with an accuracy of around 1 mm, using point gauges fixed or mounted on a mobile carriage. Although in a steady flow and well-developed scouring, the use of a conventional point gauge to measure the scour depth yields reasonably accurate results, during the initial phase or in unsteady flow conditions [34], the point gauge is not very easy to use and not very reliable.

Moreover, the point gauge is an intrusive tool that can impact, if not handled with extreme care, deeply the results. This is the reason why, to prevent any disturbance effect due to point gauges, the maximum scour depth has also been often measured, or checked, by means of a measuring tape glued at the pier surface. Although, in the case of the punctual measurement of the maximum scour depth, the point gauge and the measuring tape, can be considered acceptable techniques, in the case of two- or three-dimensional measurements of the evolution of the dune downstream of the obstacle new experimental techniques are urgently needed. The bed geometry around a pier is currently measured, along the channel, using (a) a dense array of fixed ultrasonic sensors which operates continuously [35–37] or (b) a single or a strip of a few ultrasonic or laser sensors attached to an automated trolley, which moves at constant speed on a rail [23,25,35,38–41]. The first approach guarantees a series of synchronous measurements of the bed surface, but it is certainly very expensive and highly intrusive. The second approach, although it may be very effective for developed scour holes, does not guarantee adequate synchronicity of the measures in the initial instants. In any case, although the accuracy of these devices is of the order of a tenth of a millimeter, they must be submerged and hence can induce undesired disturbances of the flow field and, when the instrument is immersed in shallow water, a local scour of the bad [42].

There are very few experimental works, to the authors' knowledge, that have used, often in a very pioneering way, non-intrusive methods to measure the evolution of the scour hole in live-bed or clear-water conditions [42,43]. Visconti et al. [42] proposed a new method to measure bed topography in shallow water and live-bed conditions. The methodology is based on laser and ultrasonic level transmitters used contemporaneously. The proposed measuring approach is nonintrusive and inexpensive but it can only be used in shallow water conditions. Bouratsis et al. [43] presented a new photogrammetric technique for the three-dimensional measurement, without interruption and at high resolution, of the bed topography in scouring experiments. The technique is based on the use of (a) two cameras recording the sediment bed during its evolution, (b) a number of algorithms for camera calibration, image rectification, and stereo-triangulation. Muller et al. [44] used the Moiré effect to map surface contours of the scour development around physical models of a railway bridge across River Rhine. The evolution of the scour was obtained by comparing the initial with the final fringe image. Finally, Chourasiya et al. [45] explored the potential of the Kinect sensor for continuous 3-D bed-profile measurements. They showed that the method is inexpensive, non-intrusive, and can provide continuous 3-D bed profiles without requiring expensive cameras or sophisticated image

analysis. According to the authors the method, that can operate only on small areas, has some limitations due to the roughness of the water surface, high turbidity, illuminance and specular reflection from the target surface.

The objective of this study is to present a new method, easy to use, inexpensive and non-intrusive, for continuous acquisition of the 2-D temporal variation of the scour hole shape around a cylindrical bridge pier for uniform sediment and steady clear-water flow. The technique is based on the use of a continuous-wave laser source and a camera. In particular, the green beam emitted by the laser source is refracted by a cylindrical lens to create a vertical laser sheet, parallel to the channel walls, and crossing radially the Plexiglas pier. The camera is placed laterally to the flume and, thanks to a simple calibration methodology, acquires the evolution of the scour hole. The design idea is not completely original but is similar to that used for very expensive systems such as the PIV [46]. The differences are to be found in the large area swept by the acquisition system and in the very low cost of the instrumentation, which can cost a few hundred euros. Although in the present work the method is applied to a 2-D case, it can be easily, through the use of more laser sheets, extended to three-dimensional measurements. To show the potential of the method, four experimental tests were carried out varying only the water velocity (U) and maintaining constant the water depth (h_0), the type of sand and the diameter of the bridge pier (D). Finally, two of the most used equations for the evolution of the maximum scour depth in clear-water conditions [2,16] are compared using the data obtained in the four runs using the new technique.

2. Experimental Set-Up and Procedure

2.1. Experimental Design and Flume

The experiments were conducted in a flume, 0.50 m wide, 0.60 m deep and 12 m long glass-sided rectangular channel with 0.5% sloping, of the Hydraulic Laboratory at the Politecnico di Torino (IT). The water is recirculated in the flume using a low and constant head reservoir, and the flow is regulated by a high precision hydraulic gate placed between the reservoir and the flume. The flow rate is measured using an electromagnetic flow gauge (PROMAG W, Endress-Hauser, Reinach, Switzerland) placed on the recirculating pipe downstream the hydraulic gate.

The water, after passing through the flume, falls into the main recirculation channel of the laboratory and is sent back to the low head tank. This recirculation system, shown in Figure 1, guarantees a constant flow rate throughout the experiment. To guarantee the water level, a sluicegate is placed at the end of the flume. The erodible bed has been obtained in the central part of channel where a 3 m long test section is built placing a 0.27 m thick layer of uniform quartz sand ($\rho_s = 2650$ kg/m^3; $d_{50} = 1.25$ mm).

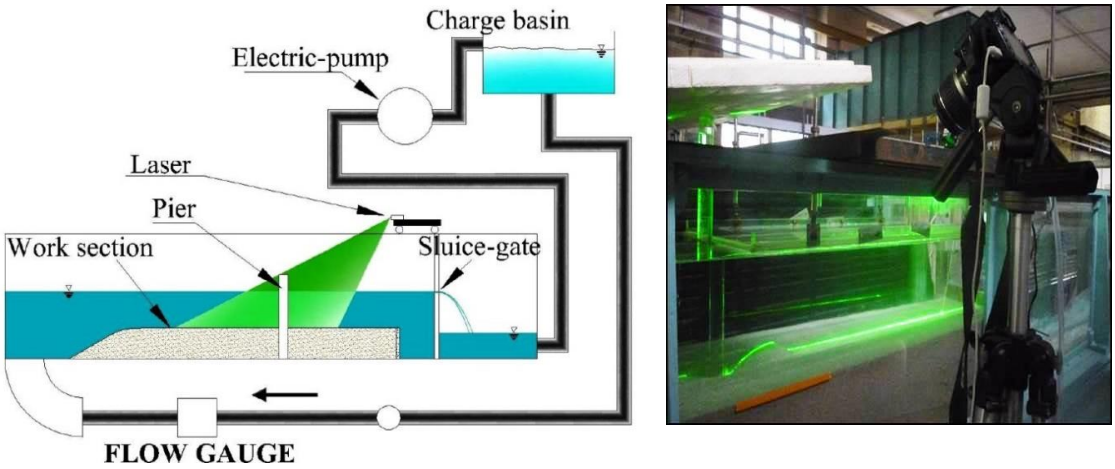


Figure 1. Schematic of the water circuit and test section. The laser sheet is highlighted in green.

A Plexiglas transparent cylinder, having a diameter $D = 32$ mm, is used as a pier and placed in the middle of the test section (Figure 2). Prior to each experiment, the sand bed on the test section was perfectly leveled. During the experiments, the water depth is kept to $h_0 = 215$ mm fixing the opening of the sluicegate. In order to avoid undesirable scouring during the unsteady state of the experiment, the flume is filled gradually and water is slowly pumped in the flume through secondary water circuits both upstream and downward of the test section. When the water level reached 215 mm the secondary pumps are stopped and the main pump is switched on.

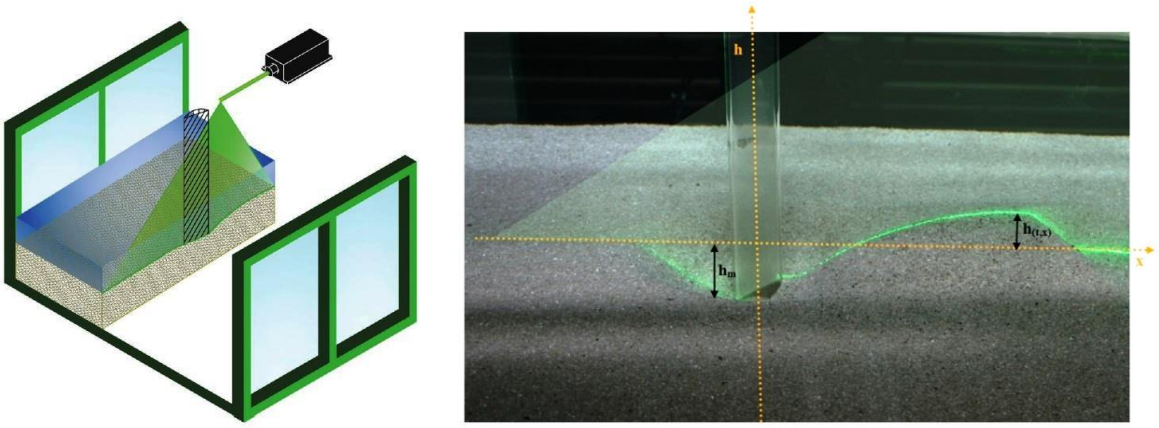


Figure 2. Schematic representation of the new technology.

Furthermore, to avoid exceeding, during the initial ramp in the flow rate, the critical velocity on the test section the tailgates remained initially closed, imposing a high water depth and low flow velocity. Only when the flow reached the wished value the tailgates is opened until the final height. This initial transient lasted only a few minutes and it didn't influence the erosive action which was generated around the pier.

2.2. Measuring System

In Figures 1 and 2 is also shown the laser sheet that is the main novelty of this work. In particular, above the flume, a continuous wave cyan line laser source (488 nm, 200 mW, Changchun New Industries Optoelectronics Tech. Co., Ltd., Changchun, Jilin, China) is installed. This type of laser is widely used in fluorescence microscopy since its wavelength activates a large number of different dyes, such as Alexa 488, eGFP, SYTO-13 DNA, Chromeo, just to name a few. In our technique, the laser source does not need to have high performance in terms of stability, coherence or beam size. A laser source of a few hundreds of mW (300–400 euros) is more than enough. The green beam emitted by the laser source is refracted by a cylindrical lens to expand the laser light along the longitudinal axis only. The result is a vertical laser sheet, parallel to the channel walls, and positioned, using a high precision carriage plate, in the middle of the channel. Furthermore, the laser sheet crossed radially the transparent Plexiglas pier and intercepts the surface of the moveable test section highlighting its geometry (Figure 3). Thanks to the fact that the laser sheet crosses the cylinder radially, its optical path is not impacted by refraction, then the laser sheet, upstream and downstream of the cylinder, is everywhere coplanar. To prevent the ripples of the water surface, created by the pile and large-scale turbulence, from altering the verticality of the laser sheet, a transparent Plexiglas slab, 1 cm wide and 60 cm long) is positioned horizontally at the level of the water surface. At the side of the flume, it is placed a digital camera "Canon EOS 400D" remote-controlled by PC set to capture an image at a set time interval. The camera is positioned so that it can frame both the upstream and downstream scour bed.

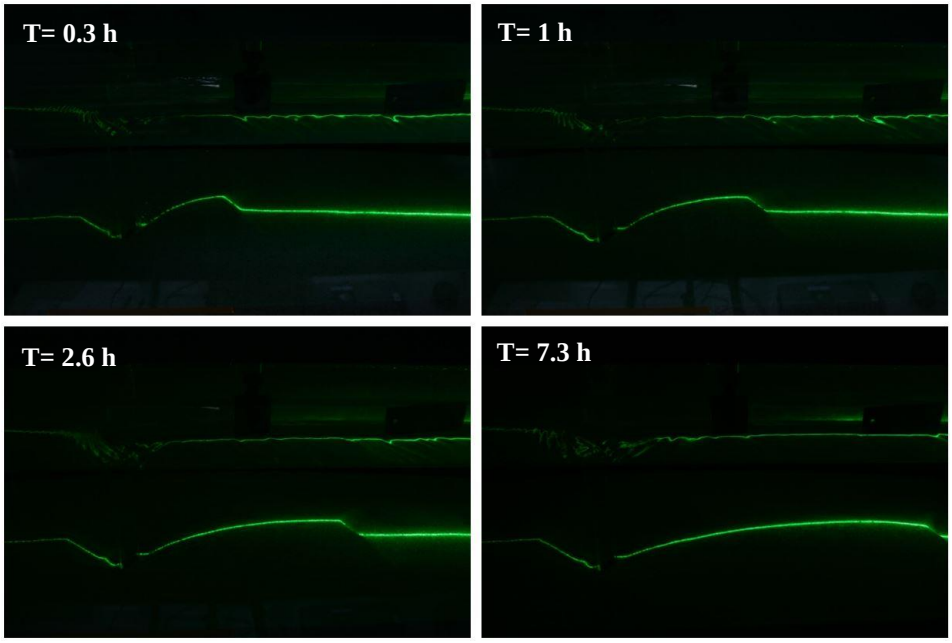


Figure 3. The profiles acquired by the camera during four moments in the experiment.

Processing this sequence of images, it is possible to obtain the scour hole evolution during the experiment. For this purpose there are three critical issues to face: (1) Identify, in each image, the footprint of the laser sheet on the sand bottom, (2) converting pixels into distances, and (3) adjusting the image distortions due to the camera lens and to the optical path of the light refracted when double-crossing two different mediums (water-glass and glass-air). The identification of the laser footprint on the bottom is a rather simple and straight forward task when the laser intensity has been correctly set and the dark conditions imposed on the channel. In particular, the laser power must not be too low, or the footprint would be unidentifiable, neither too high since it would make the track too thick and the bottom not uniquely identifiable.

Moreover, to avoid disturbances due to the color of the sand, dark conditions are met inside the channel to allow better identification of the laser footprint on the test section. In Figure 4, four photos taken during one of the tests are shown as an example. A code in MATLAB (2019a), based on the intensity of the green light (in the RGB matrix) has been appositely developed and calibrated to identify the footprint, in pixel, on every single photo.

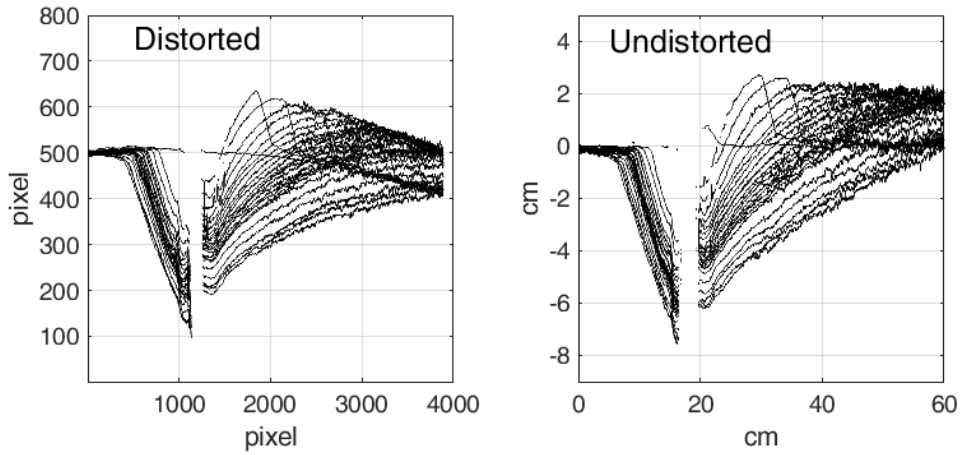


Figure 4. The bottom profiles as originally detected in the photos (distorted and in pixel), **left**, and after calibration, **right**.

2.3. Calibration and Image Processing

Distortion is inherent in all images taken through lens systems. The classical Brown lens distortion model is used to determine where any point in the distorted image would appear in the image plane if there were no lens distortion [47]. A three-millimeter sandwich panel with a core in aluminium honeycomb bonded to two skins of the aluminium panel is used as a calibration plate. This material was chosen for its lightness and rigidity. Furthermore, being entirely in aluminium, it can be used in complete immersion conditions. A checkerboard pattern (5 mm by 5 mm) was drawn on one surface of the plate using laser engraving. The calibration plate is used both for the image calibration and, at the beginning of each experimental test, as an absolute reference system in the vertical section of the laser sheet. Once the calibration plate is placed, in still water, few photos are taken without the pier. Finally, the calibration plate is removed from the flume, the pier is installed into the sad bed, and the experiment is started.

In Figure 5 the profiles of the bottom, acquired at several time instants from 0 to 24 h, are shown. As expected, the extension of the scour and its maximum depth increase as the flow rate increases. To quantitatively verify the results obtained with this new experimental technique, in the next paragraph, the comparisons between the maximum scour depth measured and that predicted by some of the most used equations are shown.

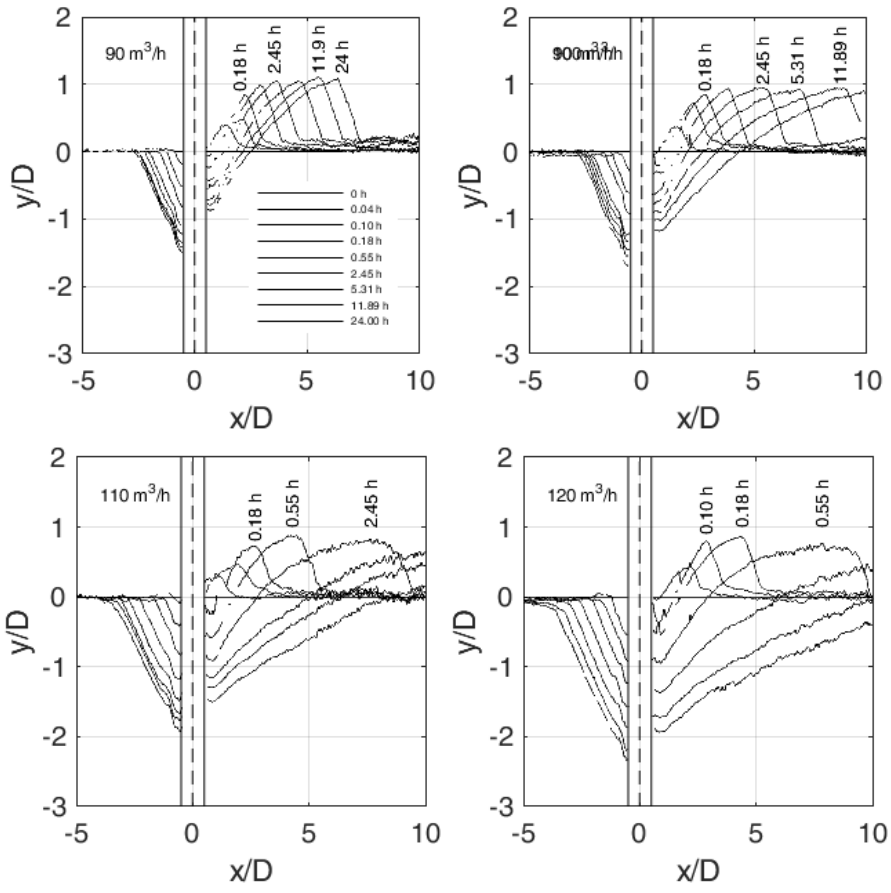


Figure 5. The profiles of the bottom for some time instants.

3. Results and Discussion

3.1. Existing Equations for Temporal Scour Depth

Several formulae and mathematical models developed for the estimation of the scour depth are still primarily based on theoretical approaches and laboratory tests [2,10,14,16,18,20,48]. This justifies

the fact that, in the last decades, a plethora of numerical and laboratory investigations have been conducted to quantify the maximum scour depth at bridge piers. From this large amount of data, several equations are available for estimating temporal and equilibrium scour depth. Most of these investigations have been focused on equilibrium scour depth and very fewer formulae are available for estimating the temporal evolution of the scour depth [2,15,16,18,49,50]. It is not our intention to remember, in this work, all the formulations or to decide which is the best. The equations are used here to verify if the results obtained by the proposed technique align with the most reliable equations used in the past. In the present study, the temporal scour depth equations proposed by Oliveto and Hager [16] and Melville and Chiew [2] are chosen for evaluating the accuracy of our data.

Oliveto and Hager [17] proposed a scour equation that involves the scour depth z as a function of time t. They observed that the densimetric particle Froude number (F_d) is the dominant parameter controlling the scour process and can be made explicit through the following scaling relationship.

$$F_d = \frac{U}{[g(\rho_s/\rho - 1)d_{50}]^{1/2}}$$

where U is the bulk approach velocity, ρ_s and ρ are the sediment and fluid densities, g is the gravitational acceleration, and d_{50} is the median grain size. Note that F_d can also be expressed as the ratio of U and a reference velocity $U_R = [g(\rho_s/\rho - 1)d_{50}]^{1/2}$. Similarly, Oliveto and Hager [17] proposed a reference length for piers $L_R = D^{\alpha}h_0{}^{\beta}$, with $\alpha + \beta = 1$, and, consequently, a reference time $T_R = L_R/U_R$. The dimensionless depth and time of scour can be written as:

$$Z = \frac{z(t)}{L_R} = \frac{z(t)}{D^{2/3}h_0{}^{1/3}}$$

As well,

$$T = \frac{t}{T_R} = t\left[\frac{g(\rho_s/\rho - 1)d_{50}}{D^{4/3}h_0{}^{2/3}}\right]^{\frac{1}{2}}$$

With, as suggested by the authors, $\alpha = 2/3$ and $\beta = 1/3$. Finally, based on a detailed data analysis conducted by Oliveto and Hager [17], and subsequently verified using more data by Pandey et al. [19], the dimensionless scour depth variation Z can be parameterized as

$$Z = 0.068\,\sigma^{-1/2}F_d{}^{3/2}\log(T)$$

With $\sigma = (d_{84}/d_{16})^{1/2}$ as the sediment uniformity parameter.

Melville and Chiew [2] proposed a time-dependent scour depth equation built around a large dataset of experimental laboratory data and reads as follows:

$$z(t) = Z_e exp\left[-0.03\left|\frac{U}{U_C}\ln\left(\frac{t}{T_e}\right)\right|^{1.6}\right]$$

where and Z_e and T_e are respectively the equilibrium scour depth and time (in days), and U_c denote the critical velocity at the threshold condition for sediment movement defined by Lauchlan and Melville [48]. Unlike what was assumed by Oliveto and Hager [17], the expression by Melville and Chiew [2] assumes that the scouring will reach an equilibrium condition. The general expression for these two equilibrium parameters can be found in [2], in our case study the are

$$Z_e = 1.37\,D\,\frac{U}{U_C}\log\left(2.24\frac{D}{d_{50}}\right)$$

As well,

$$T_e = 48.26\frac{D}{U}\left(\frac{U}{U_C} - 0.4\right)$$

Note that, this expression for T_e is valid for a flow shallowness $h_0/D > 6$. In our case, the flow shallowness is 6.7, then the maximum scour depth, according to Melville and Chiew [2], should not depend on the water depth but, unlike the formula by Oliveto and Hager [17], only on the pier diameter, incoming velocity and sand median size.

3.2. Comparison with Existing Equations

The two equations are compared in this study with clear-water temporal scour obtained in the four runs described above. The accuracy of these equations are here checked graphically in Figure 6 where the time records of the scour depths are plotted along with the estimations from Oliveto and Hager [16], as a solid line, and Melville and Chiew [2], as dash-dot line. The inspection of this figure reveals that the equation proposed by Oliveto and Hager [16] describes the data very well when the excavation is fully developed ($t > 10$ h). Although the temporal duration of the experiments does not allow a clear picture, the scour depth, as predicted by Oliveto and Hager [16], does not seem to reach a state of equilibrium. In particular, the temporal growth of scour depth seems to be of a logarithmic type as previously predicted [16,51,52]. On the contrary, the equation by Melville and Chiew [2] best describes the data in the first part of the temporal development of the scouring process.

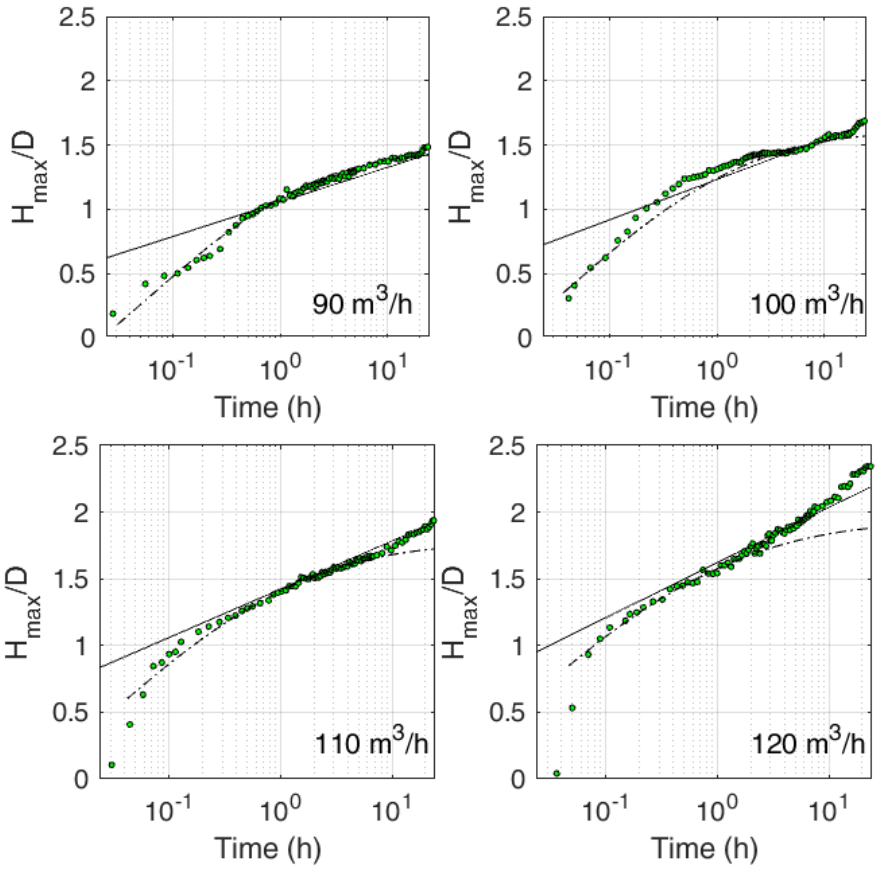


Figure 6. Time evolution of the maximum scour depth measured (**dots**) versus the estimation from Oliveto and Hager [16] (**solid line**) and Melville and Chiew [2] (**dash-dot line**).

The time evolution of the maximum scour depth measured in the four runs are shown, in the coordinates suggested by Oliveto and Hager [16], in Figure 7. As expected by the previous considerations, the inspection of Figure 7 reveals that the suggested predictor describes the scour depth time evolution quite well for $T > 4{\cdot}10^3$.

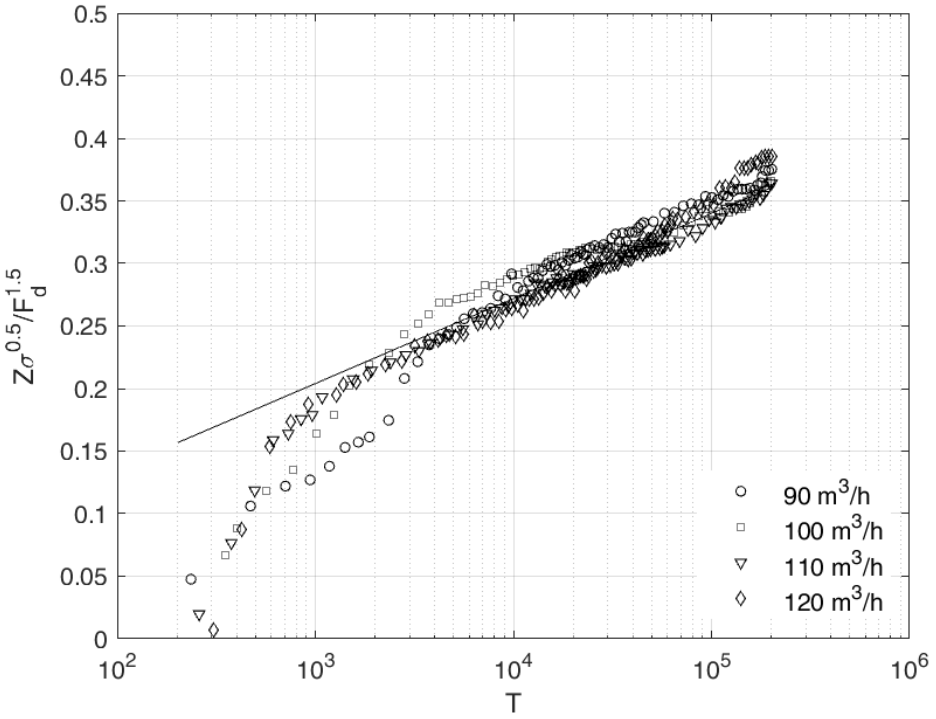


Figure 7. Time evolution of maximum scour depth measurements versus the predictors in the coordinates suggested by Oliveto and Hager [16].

4. Conclusions

A new technique for measuring the 2-D shape of an evolving scour hole has been presented. The technique is based on the use of line laser source and a commercial camera that acquires the bed evolution during the experiment. The method is described in each step, and an extended guideline for the use of the technique is provided in the paper, both in terms of experimental design and data post-processing. The intuitive methodology and the very low-cost setup make this experimental method applicable not only to scouring but also to an extensive variety of experiments where the bed is evolving in time and space. To provide a better understanding of the method and a preliminary proof of its capabilities, it has been used to carry out a short experimental measurement campaign about the time evolution of a sour hole around a bridge pier. The results have been compared with two of the most used equations for the evolution of the maximum scour depth in clear-water conditions.

Author Contributions: D.P. Conceptualization and writing-original draft; N.O.K. Investigation and Writing-review & editing.

Funding: This research received no external funding.

Acknowledgments: The writers would like to thank Emanuele Defanti for his fundamental help in the image analysis and experimental activity.

Conflicts of Interest: The authors declare no conflict of interest.

References

1. Wardhana, K.; Hadipriono, F.C. Analysis of Recent Bridge Failures in the United States. *J. Perform. Constr. Facil.* **2003**, *17*, 144–150. [CrossRef]
2. Melville, B.W.; Chiew, Y.-M. Time Scale for Local Scour at Bridge Piers. *J. Hydraul. Eng.* **1999**, *125*, 59–65. [CrossRef]
3. Johnson, P.A.; Dock, D.A. Probabilistic Bridge Scour Estimates. *J. Hydraul. Eng.* **1998**, *124*, 750–754. [CrossRef]
4. Tubaldi, E.; Macorini, L.; Izzuddin, B.A.; Manes, C.; Laio, F. A framework for probabilistic assessment of clear-water scour around bridge piers. *Struct. Saf.* **2017**, *69*, 11–22. [CrossRef]

5. Lagasse, P.F. *Reference Guide for Applying Risk and Reliability-Based Approaches for Bridge Scour Prediction*; Transportation Research Board: Washington, DC, USA, 2013; ISBN 978-0-309-28356-4.
6. Wang, C.; Yu, X.; Liang, F. A review of bridge scour: Mechanism, estimation, monitoring and countermeasures. *Nat. Hazards* **2017**, *87*, 1881–1906. [CrossRef]
7. Melville, B.W.; Coleman, S.E. *Bridge Scour*; Water Resources Publication: Highlands Ranch, CO, USA, 2000; ISBN 978-1-887201-18-6.
8. Dargahi, B. Controlling Mechanism of Local Scouring. *J. Hydraul. Eng.* **1990**, *116*, 1197–1214. [CrossRef]
9. Khosronejad, A.; Kang, S.; Sotiropoulos, F. Experimental and computational investigation of local scour around bridge piers. *Adv. Water Resour.* **2012**, *37*, 73–85. [CrossRef]
10. Manes, C.; Brocchini, M. Local scour around structures and the phenomenology of turbulence. *J. Fluid Mech.* **2015**, *779*, 309–324. [CrossRef]
11. Melville, B.W. Live-bed Scour at Bridge Piers. *J. Hydraul. Eng.* **1984**, *110*, 1234–1247. [CrossRef]
12. Toth, E.; Brandimarte, L. Prediction of local scour depth at bridge piers under clear-water and live-bed conditions: Comparison of literature formulae and artificial neural networks. *J. Hydroinform.* **2011**, *13*, 812–824. [CrossRef]
13. Ettmer, B.; Orth, F.; Link, O. Live-Bed Scour at Bridge Piers in a Lightweight Polystyrene Bed. *J. Hydraul. Eng.* **2015**, *141*, 04015017. [CrossRef]
14. Kothyari, U.C.; Hager, W.H.; Oliveto, G. Generalized Approach for Clear-Water Scour at Bridge Foundation Elements. *J. Hydraul. Eng.* **2007**, *133*, 1229–1240. [CrossRef]
15. Lança, R.M.; Fael, C.S.; Maia, R.J.; Pêgo, J.P.; Cardoso, A.H. Clear-Water Scour at Comparatively Large Cylindrical Piers. *J. Hydraul. Eng.* **2013**, *139*, 1117–1125. [CrossRef]
16. Oliveto, G.; Hager, W.H. Temporal Evolution of Clear-Water Pier and Abutment Scour. *J. Hydraul. Eng.* **2002**, *128*, 811–820. [CrossRef]
17. Kothyari, U.C.; Garde, R.C.J.; Ranga, R.K.G. Temporal Variation of Scour around Circular Bridge Piers. *J. Hydraul. Eng.* **1992**, *118*, 1091–1106. [CrossRef]
18. Oliveto, G.; Hager, W.H. Further Results to Time-Dependent Local Scour at Bridge Elements. *J. Hydraul. Eng.* **2005**, *131*, 97–105. [CrossRef]
19. Pandey, M.; Sharma, P.K.; Ahmad, Z.; Singh, U.K. Evaluation of existing equations for temporal scour depth around circular bridge piers. *Environ. Fluid Mech.* **2017**, *17*, 981–995. [CrossRef]
20. Mia, M.F.; Nago, H. Design Method of Time-Dependent Local Scour at Circular Bridge Pier. *J. Hydraul. Eng.* **2003**, *129*, 420–427. [CrossRef]
21. Sheppard, D.M.; Odeh, M.; Glasser, T. Large Scale Clear-Water Local Pier Scour Experiments. *J. Hydraul. Eng.* **2004**, *130*, 957–963. [CrossRef]
22. Oliveto, G.; Hager, W.H. Morphological Evolution of Dune-Like Bed Forms Generated by Bridge Scour. *J. Hydraul. Eng.* **2014**, *140*, 06014009. [CrossRef]
23. Chavan, R.; Kumar, B. Prediction of scour depth and dune morphology around circular bridge piers in seepage affected alluvial channels. *Environ. Fluid Mech.* **2018**, *18*, 923–945. [CrossRef]
24. Pagliara, S.; Carnacina, I. Scour and dune morphology in presence of large wood debris accumulation at bridge pier. In *River Flow 2010: Proceedings of the Fifth International Conference on Fluvial Hydraulics, Braunschweig, Germany, 8–10 June 2010*; Bundesanstalt für Wasserbau: Karlsruhe, Germany, 2010.
25. Pagliara, S.; Carnacina, I. Influence of Wood Debris Accumulation on Bridge Pier Scour. *J. Hydraul. Eng.* **2011**, *137*, 254–261. [CrossRef]
26. Pagliara, S.; Carnacina, I. Influence of large woody debris on sediment scour at bridge piers. *Int. J. Sediment Res.* **2011**, *26*, 121–136. [CrossRef]
27. Carnacina, I.; Pagliara, S.; Leonardi, N. Bridge pier scour under pressure flow conditions. *River Res. Appl.* **2019**, *35*, 844–854. [CrossRef]
28. Hill, D.F.; Younkin, B.D. PIV measurements of flow in and around scour holes. *Exp. Fluids* **2006**, *41*, 295–307. [CrossRef]
29. Zhang, H.; Nakagawa, H.; Kawaike, K.; Baba, Y. Experiment and simulation of turbulent flow in local scour around a spur dyke. *Int. J. Sediment Res.* **2009**, *24*, 33–45. [CrossRef]
30. Lu, S.-Y.; Lu, J.-Y.; Shih, D.-S. Temporal and Spatial Flow Variations over a Movable Scour Hole Downstream of a Grade-Control Structure with a PIV System. *Water* **2018**, *10*, 1002. [CrossRef]

31. Sambrook, S.G.H.; Nicholas, A.P. Effect on flow structure of sand deposition on a gravel bed: Results from a two-dimensional flume experiment: Effect on Flow Structure of Sand Deposit. *Water Resour. Res.* **2005**, *41*. [CrossRef]
32. Bottacin-Busolin, A.; Tait, S.J.; Marion, A.; Chegini, A.; Tregnaghi, M. Probabilistic description of grain resistance from simultaneous flow field and grain motion measurements: Characterizing Grain Resistance. *Water Resour. Res.* **2008**, *44*. [CrossRef]
33. González, E.P.; Marqués, J.F.; Díaz-Pache, F.S.-T.; Agudo, J.P.; Gómez, L.C. Experimental validation of a sediment transport two-dimensional depth-averaged numerical model using PIV and 3D Scanning technologies. *J. Hydraul. Res.* **2008**, *46*, 489–503. [CrossRef]
34. Chang, W.-Y.; Lai, J.-S.; Yen, C.-L. Evolution of Scour Depth at Circular Bridge Piers. *J. Hydraul. Eng.* **2004**, *130*, 905–913. [CrossRef]
35. Thorne, P.D.; Hanes, D.M. A review of acoustic measurement of small-scale sediment processes. *Cont. Shelf Res.* **2002**, *22*, 603–632. [CrossRef]
36. Branß, T.; Núñez-González, F.; Dittrich, A.; Aberle, J. A flume study to investigate the contribution of main-channel bedforms on levee formation. *E3S Web. Conf.* **2018**, *40*, 02018. [CrossRef]
37. Dahal, P.; Peng, D.; Yang, Y.L.; Sharif, H. RSS Based Bridge Scour Measurement Using Underwater Acoustic Sensor Networks. *Commun. Netw.* **2013**, *5*, 641–648. [CrossRef]
38. Lanzoni, S. Experiments on bar formation in a straight flume: 1. Uniform sediment. *Water Resour. Res.* **2000**, *36*, 3337–3349. [CrossRef]
39. Ballio, F.; Radice, A. A non-touch sensor for local scour measurements. *J. Hydraul. Res.* **2003**, *41*, 105–108. [CrossRef]
40. Lam, N.; Nathanson, M.; Lundgren, N.; Rehnström, R.; Lyon, S.W. A Cost-Effective Laser Scanning Method for Mapping Stream Channel Geometry and Roughness. *JAWRA J. Am. Water Resour. Assoc.* **2015**, *51*, 1211–1220. [CrossRef]
41. Marion, A.; Tait, S.J.; McEwan, I.K. Analysis of small-scale gravel bed topography during armoring. *Water Resour. Res.* **2003**, *39*. [CrossRef]
42. Visconti, F.; Stefanon, L.; Camporeale, C.; Susin, F.; Ridolfi, L.; Lanzoni, S. Bed evolution measurement with flowing water in morphodynamics experiments: Bed Evolution Measurement with Flowing Water. *Earth Surf. Process. Landf.* **2012**, *37*, 818–827. [CrossRef]
43. Bouratsis, P.; Diplas, P.; Dancey, C.L.; Apsilidis, N. High-resolution 3-D monitoring of evolving sediment beds. *Water Resour. Res.* **2013**, *49*, 977–992. [CrossRef]
44. Müller, G.; Mach, R.; Kauppert, K. Mapping of bridge pier scour with projection moiré. *J. Hydraul. Res.* **2001**, *39*, 531–537. [CrossRef]
45. Chourasiya, S.; Mohapatra, P.K.; Tripathi, S. Non-intrusive underwater measurement of mobile bottom surface. *Adv. Water Resour.* **2017**, *104*, 76–88. [CrossRef]
46. Wei, M.; Cheng, N.-S.; Chiew, Y.-M.; Yang, F. Vortex Evolution within Propeller Induced Scour Hole around a Vertical Quay Wall. *Water* **2019**, *11*, 1538. [CrossRef]
47. Brown, D.C. Decentering Distortion of Lenses. *Photogramm. Eng.* **1966**, *24*, 555–566.
48. Lauchlan, C.S.; Melville, B.W. Riprap Protection at Bridge Piers. *J. Hydraul. Eng.* **2001**, *127*, 412–418. [CrossRef]
49. Choi, S.-U.; Choi, B. Prediction of time-dependent local scour around bridge piers: Time-dependent local scour around bridge piers. *Water Environ. J.* **2016**, *30*, 14–21. [CrossRef]
50. Yilmaz, M.; Yanmaz, A.M.; Koken, M. Clear-water scour evolution at dual bridge piers. *Can. J. Civ. Eng.* **2017**, *44*, 298–307. [CrossRef]
51. Rouse, H. Criteria for Similarity in the Transportation of Sediment. *Univ. Iowa Stud. Eng.* **1940**, *20*, 33–49.
52. Hager, W.H. Forum Article: Plunge Pool Scour: Early History and Hydraulics. *J. Hydraul. Eng.* **1998**, *124*, 1185–1187. [CrossRef]



© 2019 by the authors. Licensee MDPI, Basel, Switzerland. This article is an open access article distributed under the terms and conditions of the Creative Commons Attribution (CC BY) license (http://creativecommons.org/licenses/by/4.0/).